INTERNATIONAL JOURNAL FOR NUMERICAL METHODS IN FLUIDS
Int. J. Numer. Meth. Fluids 2010; **63**:357–373
Published online 28 May 2009 in Wiley InterScience (www.interscience.wiley.com). DOI: 10.1002/fld.2078

MHD flow and heat transfer in a thin liquid film on an unsteady stretching sheet by the homotopy analysis method

N. F. M. Noor[1], O. Abdulaziz[2] and I. Hashim[3,*,†]

[1]*Faculty of Applied Sciences and Mathematics, Universiti Industri Selangor, 45600 Bestari Jaya Selangor, Malaysia*
[2]*Department of Mathematics, Sana'a University, 1247 Sana'a, Yemen*
[3]*Centre for Modelling and Data Analysis, School of Mathematical Sciences, Universiti Kebangsaan Malaysia, 43600 Bangi Selangor, Malaysia*

SUMMARY

The magnetohydrodynamics flow and heat transfer in a thin liquid film over an unsteady elastic stretching surface are analyzed by the homotopy analysis method. A more general surface temperature is taken into consideration. The effects of various parameters in this study are discussed and presented graphically. The good agreement between the analytic series solutions and the previous numerical results shows the effectiveness of HAM to this problem. Copyright © 2009 John Wiley & Sons, Ltd.

Received 2 February 2009; Revised 30 March 2009; Accepted 4 April 2009

KEY WORDS: MHD; thin film; homotopy analysis method; unsteady stretching; heat transfer; boundary layer

1. INTRODUCTION

Fluid flows over a stretching sheet are commonly found in many manufacturing processes such as polymer extrusion, wire and fiber coating, foodstuff processing, etc. The hydrodynamics of a flow in a thin liquid film driven by an unsteady stretching surface was first considered by Wang [1]. This problem was then extended by Andersson *et al.* [2] to include the heat transfer analysis. Liu and Andersson [3] considered a more general form of the prescribed temperature variation of the stretching sheet than that considered by Andersson *et al.* [2]. Wang [4] presented analytic solutions of the exact same problem of Andersson *et al.* [2]. Other extensions of Wang's classical problem took into consideration thermocapillary effects [5–7], magnetic effect [8] and the non-Newtonian case [9–12].

*Correspondence to: I. Hashim, Centre for Modelling and Data Analysis, School of Mathematical Sciences, Universiti Kebangsaan Malaysia, 43600 Bangi Selangor, Malaysia.
†E-mail: ishak_h@ukm.my

We believe that Wang [4] is probably the first to give exact analytical solutions based on the homotopy analysis method (HAM) [13] for the flow and heat transfer in a thin liquid film driven by an unsteady stretching surface. The HAM solutions for the non-Newtonian problem considered by Andersson *et al.* [9] were presented by Wang and Pop [12]. The recent theoretical literatures on HAM are given in [14–16] and the applications of HAM and its advantages among other methods to some nonlinear differential equations have also been discussed [17–20]. Further effectiveness of HAM to other fluid flow problems has been demonstrated by many authors (cf. [21–26]).

The purpose of the present work is to extend the model in [4] to include a magnetic field and a more general surface temperature. The similarity transformation introduced by Wang [4] transforms the extent of the independent variable into a finite range of 0–1. Analytic solutions based on HAM are presented.

2. MATHEMATICAL MODEL

Consider the unsteady two-dimensional incompressible boundary layer equations of a Newtonian fluid flow in a thin liquid film with heat transfer due to the stretching motion of a horizontal elastic surface in the presence of an applied magnetic field $B=B_0/(1-\alpha t)^{1/2}$ normal to the stretching sheet:

$$\frac{\partial u}{\partial x}+\frac{\partial v}{\partial y}=0 \tag{1}$$

$$\frac{\partial u}{\partial t}+u\frac{\partial u}{\partial x}+v\frac{\partial u}{\partial y}=\nu\frac{\partial^2 u}{\partial y^2}-\frac{\sigma B^2}{\rho}u \tag{2}$$

$$\frac{\partial T}{\partial t}+u\frac{\partial T}{\partial x}+v\frac{\partial T}{\partial y}=\kappa\frac{\partial^2 T}{\partial y^2} \tag{3}$$

subject to

$$\begin{aligned} &u=U, \quad v=0, \quad T=T_s \quad \text{at } y=0\\ &\frac{\partial u}{\partial y}=\frac{\partial T}{\partial y}=0, \quad v=\frac{\partial h}{\partial t} \quad \text{at } y=h \end{aligned} \tag{4}$$

where u and v are the velocity components of the fluid in the x- and y-directions, t is the time, T is the temperature, ν is the kinematic viscosity, σ is the electrical conductivity, ρ is the density and κ is the thermal diffusivity. Furthermore, $U=bx/(1-\alpha t)$ is the stretching surface velocity with b and α are both positive constants. The temperature of the surface of the elastic sheet is assumed to vary both along the sheet and with time in accordance with

$$T_s=T_o-T_{\text{ref}}\frac{dx^{r_1}}{\nu}(1-\alpha t)^{-r_2}$$

where T_o is the temperature at the slit, T_{ref} is the constant reference temperature for all $t<1/\alpha$, r_1 and r_2 are the positive power indices, d is the positive constant of proportionality with dimension (length$^{2-r_1}$ time^{-1}) and $h(t)$ is the uniform thickness of the liquid film. The surface of the planar

DOI: 10.1002/fld

liquid film is assumed to be smooth and free of surface waves while the viscous shear stress and the heat flux are assumed to be vanished at the adiabatic free surface.

The similarity transformations are given as

$$\psi = \beta x \left[\frac{vb}{1-\alpha t}\right]^{1/2} f(\eta) \tag{5}$$

$$T = T_o - T_{\text{ref}} \left[\frac{dx^{r_1}}{v(1-\alpha t)^{r_2}}\right] \theta(\eta) \tag{6}$$

$$\eta = \frac{1}{\beta}\left[\frac{b}{v(1-\alpha t)}\right]^{1/2} y \tag{7}$$

where (6) previously employed by Liu and Andersson [3], β is the dimensionless film thickness and $\psi(x, y)$ is the stream function defined by

$$u = \frac{\partial \psi}{\partial y} = \frac{bx}{1-\alpha t} f'(\eta) \tag{8}$$

$$v = -\frac{\partial \psi}{\partial x} = -\left(\frac{vb}{1-\alpha t}\right)^{1/2} \beta f(\eta) \tag{9}$$

which satisfies the continuity equation (1). Consequently, Equations (1)–(4) are transformed to the following nonlinear boundary value problem:

$$f''' + \gamma\left[ff'' - \frac{1}{2}S\eta f'' - (f')^2 - (S+Ma)f'\right] = 0 \tag{10}$$

$$\frac{1}{Pr}\theta'' + \gamma\left(f\theta' - r_1 f'\theta - \frac{1}{2}S\eta\theta' - r_2 S\theta\right) = 0 \tag{11}$$

subject to

$$f(0) = 0, \quad f'(0) = 1, \quad \theta(0) = 1 \tag{12}$$

$$f(1) = \tfrac{1}{2}S, \quad f''(1) = 0, \quad \theta'(1) = 0 \tag{13}$$

where primes denote differentiation with respect to η, $Ma = \sigma {B_0}^2/\rho b$ is the parameter that reflects electrically conducting fluid with magnetic field or the Hartman number, $S = \alpha/b$ is the dimensionless measure of unsteadiness, $Pr = v/\kappa$ is the Prandtl number and the dimensionless film thickness $\gamma = \beta^2$ is to be determined.

The physical quantities of interest are the skin friction coefficient and the local Nusselt number which are defined as

$$C_f = \frac{\tau_w}{\rho U^2/2}, \quad Nu_x = \frac{xq_w}{\kappa T_{\text{ref}}}$$

respectively, where the skin friction τ_w and heat transfer from the sheet, q_w are given by

$$\tau_w = \mu\left(\frac{\partial u}{\partial y}\right)_{y=0}, \quad q_w = -\kappa\left(\frac{\partial T}{\partial y}\right)_{y=0}$$

DOI: 10.1002/fld

with μ and κ being the dynamic viscosity and thermal conductivity, respectively. Hence, the expressions for the skin friction and the rate of heat transfer for general magnetohydrodynamics (MHD) flow within a thin film are written as

$$\frac{1}{2}C_f Re_x^{1/2} = \frac{1}{\beta} f''(0) \tag{14}$$

$$Nu_x Re_x^{-1/2} = \frac{dx^{r_1}}{\beta v(1-\alpha t)^{r_2}} \theta'(0) \tag{15}$$

where $Re_x = Ux/v$ is the local Reynolds number. In Wang [4], when $d = b/2, r_1 = 2$ and $r_2 = \frac{3}{2}$ in (15), the expression of the heat flux becomes

$$2Nu_x Re_x^{-3/2} = \frac{1}{\beta(1-\alpha t)^{1/2}} \theta'(0)$$

3. SOLUTION APPROACH

In HAM [13], it is assumed that $f(\eta)$ and $\theta(\eta)$ can be expressed, using the set of base functions $\{\eta^m | m = 0, 1, 2, \ldots\}$, as

$$f(\eta) = \sum_{m=0}^{+\infty} a_m \eta^m \tag{16}$$

$$\theta(\eta) = \sum_{m=0}^{+\infty} c_m \eta^m \tag{17}$$

where a_m and c_m are constants. Under the rule of solution expression denoted by (16) and (17) subject to the boundary condition (13), it is straightforward to choose

$$f_0(\eta) = \eta + \frac{3S-6}{4}\eta^2 + \frac{2-S}{4}\eta^3 \tag{18}$$

$$\theta_0(\eta) = 1 \tag{19}$$

as the initial guesses of $f(\eta)$ and $\theta(\eta)$. The auxiliary linear operators $\mathscr{L}_f = \partial^3/\partial\eta^3$ and $\mathscr{L}_\theta = \partial^2/\partial\eta^2$ are chosen with the properties

$$\mathscr{L}_f[C_1 + C_2\eta + C_3\eta^2] = 0 \tag{20}$$

$$\mathscr{L}_\theta[C_1 + C_2\eta] = 0 \tag{21}$$

where C_1, C_2 and C_3 are constants of integration. From Equations (10) and (11), the nonlinear operators are defined as

$$\mathscr{N}_f[F(\eta;q), \Gamma(q)] = F''' + \Gamma\left(FF'' - \frac{1}{2}S\eta F'' - (F')^2 - (S+Ma)F'\right) \tag{22}$$

$$\mathscr{N}_\theta[F(\eta;q), \Theta(\eta;q), \Gamma(q)] = \frac{1}{Pr}\Theta'' + \Gamma\left(F\Theta' - r_1 F'\Theta - \frac{1}{2}S\eta\Theta' - r_2 S\Theta\right) \tag{23}$$

DOI: 10.1002/fld

where $F(\eta;q)$ and $\Theta(\eta;q)$ are both unknown functions of η and q while Γ is a function dependent on q. Here, prime denotes differentiation with respect to η. Let $\hbar_f$ and $\hbar_\theta$ denote the non-zero auxiliary parameters whereas H_f and H_θ are non-zero auxiliary functions, respectively. Then the zero-order deformation equation can be constructed as

$$(1-q)\mathscr{L}_f[F(\eta;q)-f_0(\eta)]=q\hbar_f H_f \mathscr{N}_f[F(\eta;q),\Gamma(q)] \tag{24}$$

$$(1-q)\mathscr{L}_\theta[\Theta(\eta;q)-\theta_0(\eta)]=q\hbar_\theta H_\theta \mathscr{N}_\theta[F(\eta;q),\Theta(\eta;q),\Gamma(q)] \tag{25}$$

subject to the boundary conditions

$$F(0;q)=0, \quad F'(0;q)=1, \quad \Theta(0;q)=1 \tag{26}$$

$$F(1;q)=\tfrac{1}{2}S, \quad F''(1;q)=0, \quad \Theta'(1;q)=0 \tag{27}$$

where $q\in[0,1]$ is an embedding parameter. From (18)–(19), it is straightforward to show that when $q=0$, the solutions of (24)–(27) are

$$F(\eta;0)=f_0(\eta), \quad \Theta(\eta;0)=\theta_0(\eta) \tag{28}$$

Since $\hbar_f,\hbar_\theta\neq 0$ and $H_f, H_\theta\neq 0$ when $q=1$, Equations (24)–(27) are equivalent to Equations (10)–(13), respectively, provided

$$F(\eta;1)=f(\eta), \quad \Theta(\eta;1)=\theta(\eta), \quad \Gamma(1)=\gamma \tag{29}$$

Thus, as q increases from 0 to 1, $F(\eta;q)$ and $\Theta(\eta;q)$ vary from the initial guesses $f_0(\eta)$ and $\theta_0(\eta)$ to the solutions $f(\eta)$ and $\theta(\eta)$ of Equations (10)–(13), respectively. Hence, does Γ from the initial guess

$$\Gamma(0)=\gamma_0 \tag{30}$$

to the time-scale parameter γ. By the Maclaurin series and using (28) and (30), $F(\eta;q)$, $\Theta(\eta;q)$ and $\Gamma(q)$ can be expanded as series of q,

$$F(\eta;q)=f_0(\eta)+\sum_{m=1}^{+\infty} f_m(\eta)q^m \tag{31}$$

$$\Theta(\eta;q)=\theta_0(\eta)+\sum_{m=1}^{+\infty} \theta_m(\eta)q^m \tag{32}$$

$$\Gamma(q)=\gamma_0+\sum_{m=1}^{+\infty} \gamma_m q^m \tag{33}$$

where

$$f_m(\eta)=\frac{1}{m!}\left[\frac{\partial^m F(\eta;q)}{\partial q^m}\right]_{q=0} \tag{34}$$

$$\theta_m(\eta)=\frac{1}{m!}\left[\frac{\partial^m \Theta(\eta;q)}{\partial q^m}\right]_{q=0} \tag{35}$$

DOI: 10.1002/fld

$$\gamma_m = \frac{1}{m!}\left[\frac{\partial^m \Gamma(q)}{\partial q^m}\right]_{q=0} \tag{36}$$

Therefore, using (29) we have

$$f(\eta) = f_0(\eta) + \sum_{m=1}^{+\infty} f_m(\eta) \tag{37}$$

$$\theta(\eta) = \theta_0(\eta) + \sum_{m=1}^{+\infty} \theta_m(\eta) \tag{38}$$

$$\gamma = \gamma_0 + \sum_{m=1}^{+\infty} \gamma_m \tag{39}$$

Differentiating Equations (24) and (25) m times with respect to q, then setting $q=0$ and finally dividing them by $m!$, the so-called mth-order deformation equations are obtained as follows:

$$\mathscr{L}_f[f_m(\eta) - \chi_m f_{m-1}(\eta)] = \hbar_f H_f(\eta)\mathscr{R}_{1,m}(\eta) \tag{40}$$

$$\mathscr{L}_\theta[\theta_m(\eta) - \chi_m \theta_{m-1}(\eta)] = \hbar_\theta H_\theta(\eta)\mathscr{R}_{2,m}(\eta) \tag{41}$$

subject to the boundary conditions

$$f_m(0) = 0, \quad f'_m(0) = 0, \quad \theta_m(0) = 0 \tag{42}$$

$$f_m(1) = 0, \quad f''_m(1) = 0, \quad \theta'_m(1) = 0 \tag{43}$$

for $m \geqslant 1$, where

$$\mathscr{R}_{1,m}(\eta) = f'''_{m-1} + \sum_{n=0}^{m-1} \gamma_{m-1-n} \sum_{i=0}^{n} (f_i f''_{n-i} - f'_i f'_{n-i}) - \frac{1}{2} S\eta \sum_{n=0}^{m-1} \gamma_n f''_{m-1-n} - (S + Ma) \sum_{n=0}^{m-1} \gamma_n f'_{m-1-n} \tag{44}$$

$$\mathscr{R}_{2,m}(\eta) = \frac{1}{\mathrm{Pr}}\theta''_{m-1} + \sum_{n=0}^{m-1} \gamma_{m-1-n} \sum_{i=0}^{n} (f_i \theta'_{n-i} - r_1 f'_{n-i}\theta_i) - \frac{1}{2} S\eta \sum_{n=0}^{m-1} \gamma_n \theta'_{m-1-n} - r_2 S \sum_{n=0}^{m-1} \gamma_n \theta_{m-1-n} \tag{45}$$

and

$$\chi_m = \begin{cases} 1, & m > 1 \\ 0, & m = 1 \end{cases}$$

DOI: 10.1002/fld

The solutions of (40) and (41) can be expressed as

$$f_m(\eta)=\int_0^\eta\int_0^\eta\int_0^\eta \hbar_f H_f(s)\mathscr{R}_{1,m}(s)\,\mathrm{d}s\,\mathrm{d}s\,\mathrm{d}s+\chi_m f_{m-1}+C_1+C_2\eta+C_3\eta^2 \tag{46}$$

$$\theta_m(\eta)=\int_0^\eta\int_0^\eta \hbar_\theta H_\theta(s)\mathscr{R}_{2,m}(s)\,\mathrm{d}s\,\mathrm{d}s+\chi_m\theta_{m-1}+C_1+C_2\eta \tag{47}$$

Hence, the mth-order approximation of $f(\eta)$, $\theta(\eta)$ and γ are given by

$$f(\eta)\approx\sum_{n=0}^{m} f_n(\eta) \tag{48}$$

$$\theta(\eta)\approx\sum_{n=0}^{m} \theta_n(\eta) \tag{49}$$

$$\gamma\approx\sum_{n=0}^{m-1} \gamma_n \tag{50}$$

where γ_n can be obtained by solving the equation $f_{n+1}(\eta)$ with respect to the boundary conditions $f_{n+1}(1)=0$ and $f'_{n+1}(1)=0$ of (43) $\forall n\geqslant 0$ simultaneously.

4. RESULTS AND DISCUSSION

The algorithm for solving Equations (40)–(43) is coded in the computer algebra package Maple where Maple's built-in `dsolve` procedure for ordinary differential equations is employed. The auxiliary functions H_f and H_θ in Equations (40) and (41) are set to be equal to 1 in all calculations done in this paper. It is found that the solutions for (40)–(43) can be expressed by

$$f_m(\eta)=\sum_{k=2}^{4m+3} a_{m,k}\eta^k,\quad \theta_m(\eta)=\sum_{k=1}^{4m} b_{m,k}\eta^k \tag{51}$$

for $m\geqslant 1$, where $a_{m,k}$ and $b_{m,k}$ are coefficients of η^k in the series, which can be obtained recursively for $m=1,2,3,\ldots$ using

$$a_{0,1}=1,\quad a_{0,2}=\frac{3S-6}{4},\quad a_{0,3}=\frac{2-S}{4},\quad b_{0,0}=1 \tag{52}$$

given by the initial guesses (18) and (19). When $m=1$, the following analytic solutions are obtained:

$$f_1(\eta)=\sum_{k=2}^{7} a_{1,k}\eta^k,\quad \theta_1(\eta)=\sum_{k=1}^{4} b_{1,k}\eta^k,\quad \gamma_0=\frac{105(2-S)}{2R} \tag{53}$$

where

$$a_{1,2}=\frac{3\hbar_f(25S^3-94S^2+14S^2Ma-56Ma(S-1)+76S+24)}{16R} \tag{54}$$

$$a_{1,3}=\frac{-3\hbar_f(12S^3-44S^2+7S^2Ma-28Ma(S-1)+32S+16)}{4R} \tag{55}$$

DOI: 10.1002/fld

$$a_{1,4}=\frac{105\hbar_f(3S^3-10S^2+2S^2Ma-35Ma(S-1)+4S+8)}{64R} \tag{56}$$

$$a_{1,5}=\frac{-21\hbar_f(S^3+2S^2+2S^2Ma-8Ma(S-1)-20S+24)}{64R} \tag{57}$$

$$a_{1,6}=\frac{-21\hbar_f(S^3-6S^2+12S-8)}{64R} \tag{58}$$

$$a_{1,7}=\frac{3\hbar_f(S^3-6S^2+12S-8)}{64R} \tag{59}$$

$$b_{1,1}=\frac{-105\hbar_\theta(r_1+2r_2)(S-2)S}{4R} \tag{60}$$

$$b_{1,2}=\frac{105\hbar_\theta(r_1+r_2S)(S-2)}{4R} \tag{61}$$

$$b_{1,3}=\frac{105\hbar_\theta r_1(S-2)^2}{8R} \tag{62}$$

$$b_{1,4}=\frac{-105\hbar_\theta r_1(S-2)^2}{32R} \tag{63}$$

with $R=36S^2+21SMa-25S-7Ma+11$. When $Ma=0$ is considered, the definition of R reduces to $R=36S^2-25S+11$ of Wang [4].

First we note that the HAM analytic solutions contain two non-zero auxiliary parameters $\hbar_f$ and $\hbar_\theta$ which can be used to adjust and control the convergence of the series solutions. The proper values of $\hbar_f$ and $\hbar_\theta$ can be determined by means of the so-called $\hbar$-curve [13]. Figure 1 shows the variations of $\gamma=\beta^2$ with $\hbar_f$ in the case $S=0.8$, $r_1=2$, $r_2=\frac{3}{2}$, $Ma=0$ and $Ma=1$ using 7th- and 10th-order of HAM approximation. The particular case $Ma=0$ recovers the results of

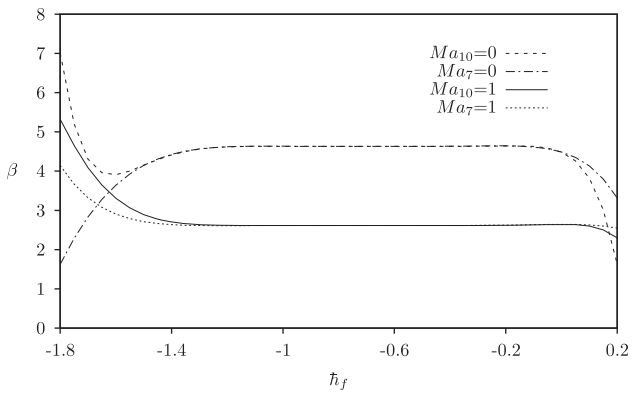

Figure 1. Variation of $\gamma=\beta^2$ with $\hbar_f$ using 7th- and 10th-order HAM approximation for the case $S=0.8$, $r_1=2$, $r_2=\frac{3}{2}$ when $Ma=0$ (Wang [4]) and $Ma=1$ (present study), respectively.

DOI: 10.1002/fld

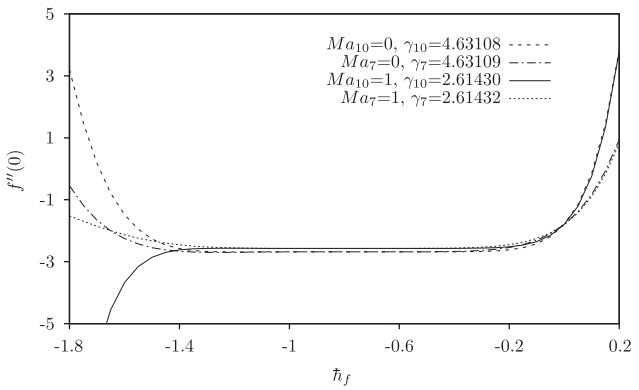

Figure 2. The $\hbar_f$-curves of $f''(0)$ using 7th- and 10th-order HAM approximation for the case $S=0.8$, $r_1=2$, $r_2=\frac{3}{2}$ when $Ma=0$ and 1, respectively.

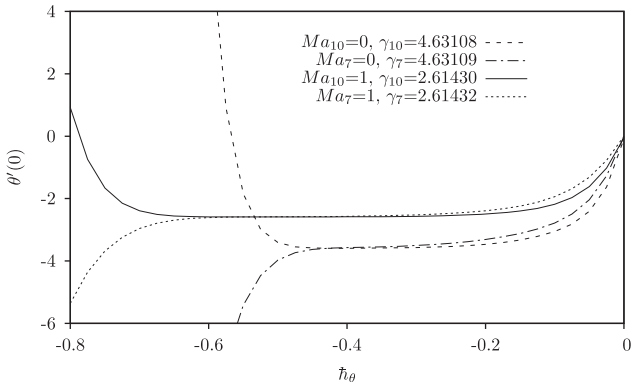

Figure 3. The $\hbar_\theta$-curves of $\theta'(0)$ using 7th- and 10th-order HAM approximation ($\hbar_f=-0.6$) for the case $S=0.8$, $r_1=2$, $r_2=\frac{3}{2}$, $Pr=1$ when $Ma=0$ and 1, respectively.

Wang [4]. It is seen that convergent results can be obtained by choosing a value for $\hbar_f$ in the range $-1.1\leqslant\hbar_f\leqslant-0.2$ for the case $S=0.8$, $Ma=0$ if 7th- and 10th-order HAM approximation are used. For example, when $\hbar_f=-0.6$, we obtain $f''(0)=-2.68094$ and $\gamma=4.63108$ which agree with the results of Wang [4] and Andersson *et al.* [2]. The $\hbar_f$-curves of $f''(0)$ are graphed in Figure 2 which simply shows that when the auxiliary parameter $\hbar_f$ is properly chosen between -1.3 and -0.3 for $r_1=2$, $r_2=\frac{3}{2}$, $S=0.8$, $Pr=1$, $Ma=0$ and $Ma=1$, the rate and region for the convergent values of $f''(0)$ can easily be attained. The appropriate choice of the auxiliary parameter $\hbar_\theta$ to maintain the convergent rate and region of $\theta'(0)$ is acquired in the range $-0.45<\hbar_\theta<-0.35$ when $Ma=0$ and $-0.60<\hbar_\theta<-0.35$ when $Ma=1$ as presented by the $\hbar_\theta$-curves in Figure 3 for $r_1=2$, $r_2=\frac{3}{2}$, $S=0.8$, $\hbar_f=-0.6$ and $Pr=1$. Based on Figures 1–3, HAM 10th-order approximation provides slightly longer range for the convergence-control parameter $\hbar$ [15] rather than the 7th-order HAM approximation. Table I presents the effect of the unsteadiness parameter S on β and $f''(0)$ for the case $Ma=0$. Comparisons of the values of $\beta=\gamma^{1/2}$, $f'(1)$, $f''(1)$ and $f''(0)$ when $r_1=2$,

DOI: 10.1002/fld

Table I. Comparison of the dimensionless film thickness, β, and the surface velocity gradient, $f''(0)$, using 10th-order HAM approximation ($\hbar_f = -0.6$), when $Ma = 0$, $r_1 = 2$, $r_2 = \frac{3}{2}$ and for several values of S.

	Present work			Wang [4]		
S	β	$f''(0)$	$f''(0)/\beta$	β	$f''(0)$	$f''(0)/\beta$
0.8	2.15199	−2.68094	−1.245796	2.15199	−2.68094	−1.245796
1.0	1.54362	−1.97238	−1.277763	1.54362	−1.97238	−1.277763
1.2	1.12778	−1.44263	−1.279177	1.12778	−1.44263	−1.279177
1.4	0.821032	−1.012780	−1.233545	0.821032	−1.012784	−1.233550
1.6	0.576173	−0.642397	−1.114938	0.576173	−0.642397	−1.114938
1.8	0.356389	−0.309137	−0.867415	0.356389	−0.309137	−0.867415

Table II. Comparison of the free surface temperature, $\theta(1)$, and heat flux from the liquid film to the stretching sheet, $-\theta'(0)$, using 10th-order HAM approximation, when $Ma = 0$, $r_1 = 2$, $r_2 = \frac{3}{2}$ and for several values of Pr.

	Present work			Wang [4]		
Pr	$\theta(1)$	$-\theta'(0)$	$-\theta'(0)/\beta$	$\theta(1)$	$-\theta'(0)$	$-\theta'(0)/\beta$
$S = 0.8$, $\hbar_f = -0.6$ and $\beta = 2.15199$						
0.01	0.960480	0.090474	0.042042	0.960480	0.090474	0.042042
0.10	0.692533	0.756162	0.351378	0.692533	0.756162	0.351378
1.00	0.097881	3.593268	1.669742	0.097884	3.595970	1.670998
2.00	0.024945	5.226744	2.428796	0.024941	5.244150	2.436884
3.00	0.008786	6.382744	2.965973	0.008785	6.514440	3.027170
$S = 1.2$, $\hbar_f = -1.0$ and $\beta = 1.12778$						
0.01	0.982331	0.037734	0.033459	0.982331	0.037734	0.033459
0.10	0.843622	0.343931	0.304963	0.843622	0.343931	0.304963
1.00	0.286712	1.999224	1.772707	0.286717	1.999590	1.773032
2.00	0.128031	2.975320	2.638210	0.128124	2.975450	2.638324
3.00	0.067423	3.693560	3.275071	0.067658	3.698830	3.279744

$r_2 = \frac{3}{2}$ and several values of Ma are shown in Table III. The method used in Abel *et al.* [8] is the fourth-order Runge–Kutta with shooting. The results in Tables I–III confirm the validity of our codes.

Further numerical results of the skin friction and heat transfer values for MHD thin film flow are tabulated in Tables IV–VI when the unsteadiness parameter S, the Hartman number Ma and the auxiliary parameter $\hbar_f$ are varied, respectively. It can be summarized that when S (Table IV) or Ma (Table V) increases, the film thickness $\beta = \gamma^{1/2}$ and the wall heat flux $-\theta'(0)$ decrease, whereas the skin friction $f''(0)$ and the free temperature $\theta(1)$ values escalate. Based on Table VI, the convergent values of $\beta = \gamma^{1/2}$ and $f''(0)$ can be generated when the auxiliary parameter $\hbar_f$ is between -0.4 and -1.2 for both cases of $r_1 = 2$, $r_2 = \frac{3}{2}$, $S = 1.0$, $Pr = 1$, $\hbar_\theta = -0.5$ and $r_1 = r_2 = 1$, $S = 0.8$, $Pr = 1$, $\hbar_\theta = -0.4$. Variations of the wall heat flux $-\theta'(0)$ and the free surface temperature

DOI: 10.1002/fld

Table III. Comparison of the values of $\beta=\gamma^{1/2}$, $f'(1)$, $f''(1)$ and $f''(0)$ when $r_1=2$, $r_2=\frac{3}{2}$ and the Hartman number Ma is varied.

	Present work				Abel *et al.* [8]		
Ma	β	$f''(0)$	$f'(1)$	$f''(1)$	β	$f'(1)$	$f''(1)$
$S=0.8$ (10th-order of HAM, $\hbar_f=-0.6$)							
0	2.151994	−2.680944	0.187840	0.000000	2.151990	0.187840	0.000000
1	1.616881	−2.569836	0.179716	0.000000	1.616880	0.179716	0.000000
2	1.350881	−2.526794	0.176487	0.000000	1.350880	0.176488	0.000000
3	1.184198	−2.503884	0.174751	0.000000	1.184197	0.174751	0.000000
4	1.067176	−2.489651	0.173665	0.000000	1.067175	0.173665	0.000000
5	0.979193	−2.479948	0.172922	0.000000	0.979192	0.172922	0.000000
6	0.909924	−2.472908	0.172382	0.000000	0.909925	0.172381	0.000000
7	0.853552	−2.467566	0.171971	0.000000	0.853552	0.171971	0.000000
8	0.806513	−2.463375	0.171648	0.000000	0.806512	0.171648	0.000000
$S=1.2$ (10th-order of HAM, $\hbar_f=-1.0$)							
0	1.127781	−1.442625	0.427547	0.000000	1.127780	0.427548	0.000000
1	0.903879	−1.417580	0.425050	0.000000	0.903878	0.425050	0.000000
2	0.775796	−1.405663	0.423848	0.000000	0.775795	0.423849	0.000000
3	0.690239	−1.398695	0.423141	0.000000	0.690238	0.423142	0.000000
4	0.627910	−1.394122	0.422676	0.000000	0.627910	0.422676	0.000000
5	0.579900	−1.390891	0.422346	0.000000	0.579900	0.422346	0.000000
6	0.541450	−1.388486	0.422100	0.000000	0.541450	0.422100	0.000000
7	0.509757	−1.386626	0.421910	0.000000	0.509757	0.421909	0.000000
8	0.483049	−1.385146	0.421758	0.000000	0.483048	0.421759	0.000000

Table IV. Variation of $\beta=\gamma^{1/2}$, $f''(0)$, $\theta(1)$ and $-\theta'(0)$ using 10th-order HAM approximation when $Ma=1$, $Pr=1$ and S is varied.

S	β	$f''(0)$	$\theta(1)$	$-\theta'(0)$
$r_1=2$, $r_2=\frac{3}{2}$, $\hbar_f=-0.5$, $\hbar_\theta=-0.5$				
0.6	2.264512	−3.528709	0.133532	3.459299
0.8	1.616884	−2.569610	0.214130	2.587477
1.0	1.200886	−1.917629	0.306767	1.983810
1.2	0.903880	−1.417470	0.412687	1.510059
1.4	0.674623	−1.002432	0.533097	1.103694
$r_1=r_2=1$, $\hbar_f=-0.6$, $\hbar_\theta=-0.4$				
0.6	2.264602	−3.529004	0.236345	2.531606
0.8	1.616881	−2.569836	0.341740	1.875512
1.0	1.200884	−1.917781	0.447995	1.415288
1.2	0.903879	−1.417570	0.555961	1.053417
1.4	0.674623	−1.002490	0.665552	0.747922

values $\theta(1)$ with respect to Pr are listed in Table VII. Based on Table VII, it is noted that higher Prandtl number Pr decreases $\theta(1)$, but increases $-\theta'(0)$ for the cases of $\beta=1.200886$, $r_1=2$, $r_2=\frac{3}{2}$, $S=1.0$, $\hbar_f=\hbar_\theta=-0.5$ and $\beta=1.616881$, $r_1=r_2=1$, $S=0.8$, $\hbar_f=-0.6$, $\hbar_\theta=-0.4$.

DOI: 10.1002/fld

Table V. Variation of $\beta=\gamma^{1/2}$, $f''(0)$, $\theta(1)$ and $-\theta'(0)$ using 10th-order HAM approximation when $Pr=1$ and Ma is varied.

Ma	β	$f''(0)$	$\theta(1)$	$-\theta'(0)$
$r_1=2,\ r_2=\frac{3}{2},\ S=1,\ \hbar_f=-0.5,\ \hbar_\theta=-0.5$				
0.0	1.543619	−1.972205	0.180688	2.675102
0.5	1.340293	−1.938218	0.247614	2.268944
1.0	1.200886	−1.917629	0.306767	1.983810
2.0	1.017141	−1.893898	0.402709	1.600785
3.0	0.898195	−1.880614	0.476204	1.349512
5.0	0.748439	−1.866222	0.580365	1.033307
10.0	0.563534	−1.852052	0.720329	0.656777
50.0	0.266723	−1.837647	0.924012	0.169523
$r_1=r_2=1,\ S=0.8,\ \hbar_f=-0.6,\ \hbar_\theta=-0.4$				
0.0	2.151994	−2.680944	0.187817	2.677204
0.5	1.827355	−2.609606	0.271666	2.194358
1.0	1.616881	−2.569836	0.341740	1.875512
2.0	1.350881	−2.526794	0.449771	1.467569
3.0	1.184198	−2.503884	0.528172	1.211742
5.0	0.979193	−2.479948	0.633472	0.902848
10.0	0.731882	−2.457220	0.765332	0.554407
50.0	0.343901	−2.434916	0.939730	0.136412

Table VI. Variation of $\beta=\gamma^{1/2}$, $f''(0)$, $\theta(1)$ and $-\theta'(0)$ using 10th-order HAM approximation when $Ma=1$, $Pr=1$ and $\hbar_f$ is varied.

$\hbar_f$	β	$f''(0)$	$\theta(1)$	$-\theta'(0)$
$r_1=2,\ r_2=3/2,\ S=1,\ \hbar_\theta=-0.5$				
−0.2	1.201564	−1.884224	0.306559	1.987328
−0.4	1.200909	−1.916515	0.306766	1.983980
−0.5	1.200886	−1.917629	0.306767	1.983810
−0.6	1.200884	−1.917781	0.306765	1.983775
−0.8	1.200884	−1.917796	0.306765	1.983764
−1.0	1.200884	−1.917796	0.306767	1.983759
−1.2	1.200880	−1.917893	0.306755	1.983816
$r_1=r_2=1,\ S=0.8,\ \hbar_\theta=-0.4$				
−0.2	1.618585	−2.516008	0.341146	1.882344
−0.4	1.616920	−2.568005	0.341796	1.875913
−0.5	1.616884	−2.569610	0.341758	1.875600
−0.6	1.616881	−2.569836	0.341740	1.875512
−0.8	1.616881	−2.569858	0.341731	1.875458
−1.0	1.616859	−2.569784	0.341684	1.875502
−1.2	1.617971	−2.566599	0.343189	1.872479

The velocity and temperature profiles are presented in Figures 4 and 5 for several values of S and Ma, respectively. From Figure 4, it can be said that increasing S causes a rise in the flow velocity and temperature. In Figure 5, it is shown that the effect of Ma is small on the velocity,

DOI: 10.1002/fld

Table VII. Variation of $\theta(1)$ and $-\theta'(0)$ using 10th-order HAM approximation when $Ma=1$ and Pr is varied.

S	r_1	r_2	Pr	$\theta(1)$	$-\theta'(0)$
1	2	$\frac{3}{2}$		($\hbar_f=-0.5$, $\hbar_\theta=-0.5$)	
			0.70	0.409838	1.574313
			1.00	0.306767	1.983810
			2.00	0.138760	2.937627
			3.00	0.068549	3.520466
0.8	1	1		($\hbar_f=-0.6$, $\hbar_\theta=-0.4$)	
			0.70	0.448860	1.471605
			1.00	0.341740	1.875512
			2.00	0.155169	2.782922
			3.00	0.069292	3.299425

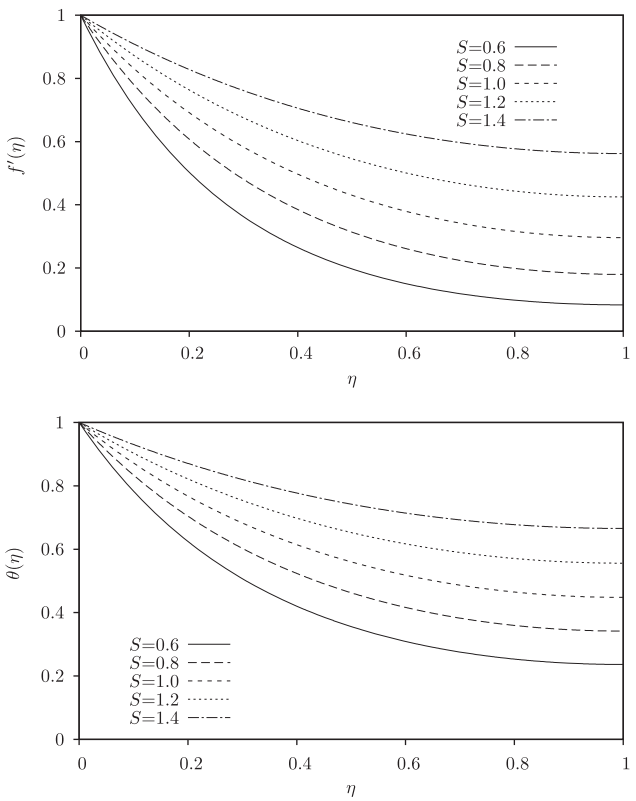

Figure 4. Effects of S on the velocity and temperature profiles using 10th-order HAM approximation ($\hbar_f=-0.6$, $\hbar_\theta=-0.4$) for the case $Ma=1$, $Pr=1$, $r_1=1=r_2=1$.

DOI: 10.1002/fld

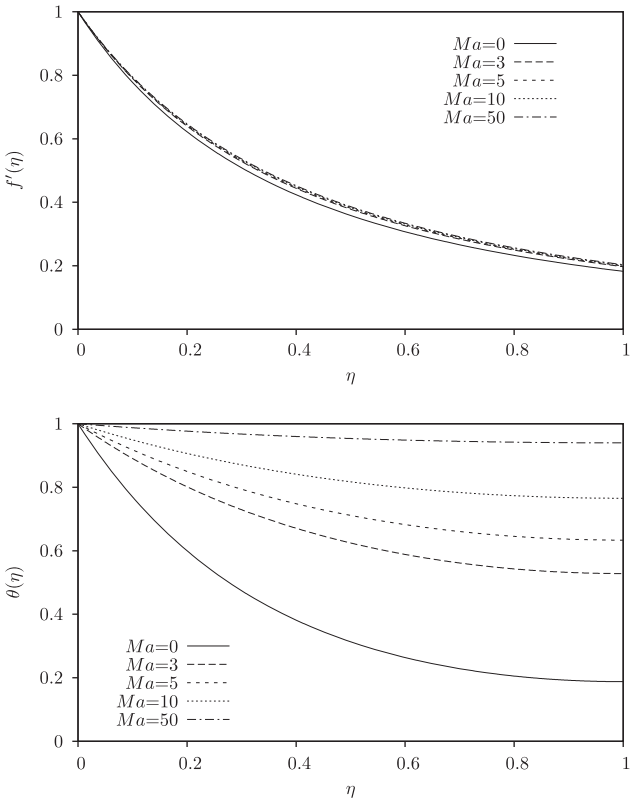

Figure 5. Effects of Ma on the velocity and temperature profiles using 10th-order HAM approximation ($\hbar_f = -0.6$, $\hbar_\theta = -0.4$) for the case $S = 0.8$, $Pr = 1$, $r_1 = 1 = r_2 = 1$.

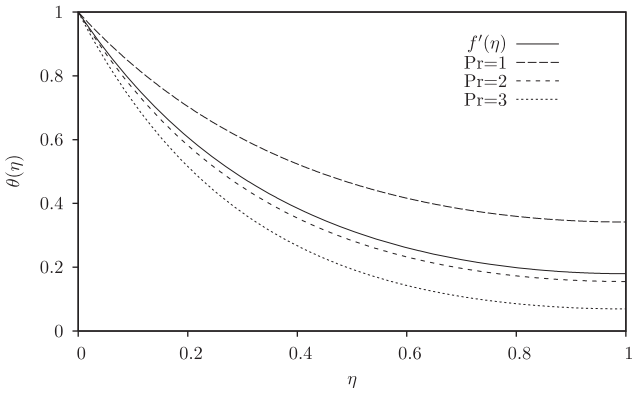

Figure 6. Effects of Pr on the temperature profiles using 10th-order HAM approximation ($\hbar_f = -0.6$, $\hbar_\theta = -0.4$) for the case $S = 0.8$, $Ma = 1$, $r_1 = 1 = r_2 = 1$.

DOI: 10.1002/fld

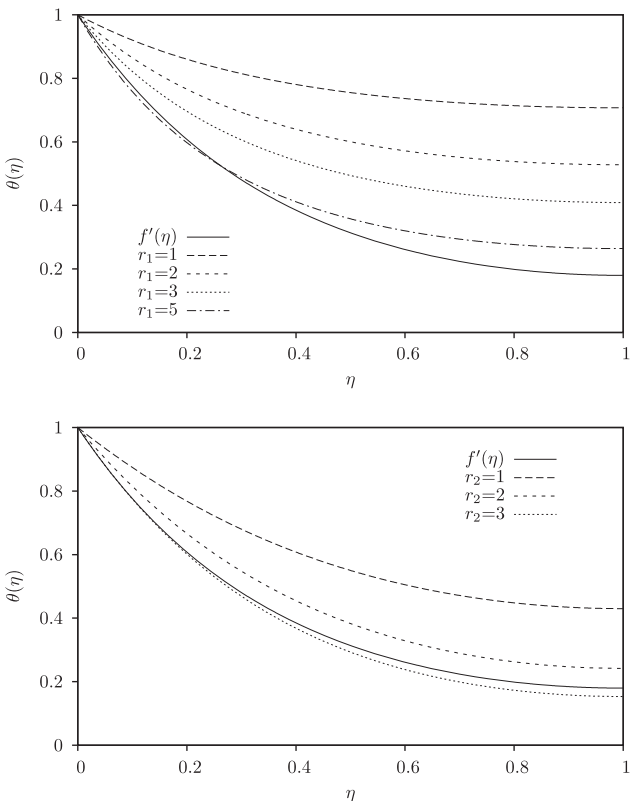

Figure 7. Effects of (a) r_1 with $r_2=0$ and (b) r_2 with $r_1=0$ on the temperature profiles using 10th-order HAM approximation ($\hbar_f=-0.6$, $\hbar_\theta=-0.4$) for the case $S=0.8$, $Ma=1$ and $Pr=1$.

whereas higher values of Ma increase the temperature. Increasing the Prandtl number will speed up the cooling as depicted in Figure 6. Moreover, the effects of the power indices r_1 and r_2 on the temperature profiles are presented for $S=0.8$, $Ma=1$, $\hbar_f=-0.6$, $\hbar_\theta=-0.4$ and $Pr=1$ in Figure 7.

5. CONCLUDING REMARKS

In this study, the MHD flow and heat transfer within a thin liquid film due to an unsteady elastic stretching sheet has been analyzed successfully using the HAM. The analytic and purely numerical solutions agree very well. Based on the cases investigated, the magnetic field parameter Ma has a small effect on the velocity, but big effect on the temperature. The power indices r_1 (r_2) have been shown to have the effect of decreasing the temperature when r_2 (r_1) is absence. Generally, higher approximation order of HAM increases the measure of convergence in the results by means of the properly chosen auxiliary parameter $\hbar$.

DOI: 10.1002/fld

REFERENCES

1. Wang CY. Liquid film on an unsteady stretching sheet. *Quarterly of Applied Mathematics* 1990; **48**:601–610.
2. Andersson HI, Aarseth JB, Dandapat BS. Heat transfer in a liquid film on an unsteady stretching surface. *International Journal of Heat and Mass Transfer* 2000; **43**:69–74.
3. Liu IC, Andersson HI. Heat transfer in a liquid film on an unsteady stretching sheet. *International Journal of Thermal Sciences* 2008; **47**:766–772.
4. Wang C. Analytic solutions for a liquid thin film on an unsteady stretching surface. *Heat and Mass Transfer* 2006; **42**:759–766.
5. Dandapat BS, Santra B, Andersson HI. Thermocapillarity in a liquid film on an unsteady stretching surface. *International Journal of Heat and Mass Transfer* 2003; **46**:3009–3015.
6. Dandapat BS, Santra B, Vajravelu K. The effects of variable fluid properties and thermocapillarity on the flow of a thin film on an unsteady stretching sheet. *International Journal of Heat and Mass Transfer* 2007; **50**:991–996.
7. Chen CH. Marangoni effects on forced convection of power-law liquids in a thin film over a stretching surface. *Physics Letters A* 2007; **370**:51–57.
8. Abel MS, Mahesha N, Tawade J. Heat transfer in a liquid film over an unsteady stretching surface with viscous dissipation in presence of external magnetic field. *Applied Mathematical and Modelling*, DOI: 10.1016/j.apm.2008.11.021.
9. Andersson HI, Aarseth JB, Braud N, Dandapat BS. Flow of a power-law fluid film on an unsteady stretching surface. *Journal of Non-Newtonian Fluid Mechanics* 1996; **62**:1–8.
10. Chen CH. Heat transfer in a power-law fluid film over a unsteady stretching sheet. *Heat and Mass Transfer* 2003; **39**:791–796.
11. Chen CH. Effect of viscous dissipation on heat transfer in a non-Newtonian liquid film over an unsteady stretching sheet. *Journal of Non-Newtonian Fluid Mechanics* 2006; **135**:128–135.
12. Wang C, Pop I. Analysis of the flow of a power-law fluid film on an unsteady stretching surface by means of homotopy analysis method. *Journal of Non-Newtonian Fluid Mechanics* 2006; **138**:161–172.
13. Liao SJ. *Beyond Perturbation*: *Introduction to the Homotopy Analysis Method*. Chapman & Hall: Boca Raton, 2004.
14. Liao SJ, Tan Y. A general approach to obtain series solutions of nonlinear differential equations. *Studies in Applied Mathematics* 2007; **119**:297–354.
15. Liao SJ. Notes on the homotopy analysis method: some definitions and theorems. *Communications in Nonlinear Science and Numerical Simulation* 2009; **14**:983–997.
16. Van Gorder RA, Vajravelu K. On the selection of auxiliary functions, operators, and convergence control parameters in the application of the homotopy analysis method to nonlinear differential equations: a general approach. *Communications in Nonlinear Science and Numerical Simulation*, DOI: 10.1016/j.cnsns.2009.03.008.
17. Abbasbandy S. The application of homotopy analysis method to solve a generalized Hirota–Satsuma coupled KdV equation. *Physics Letters A* 2007; **361**:478–483.
18. Van Gorder RA, Vajravelu K. Analytic and numerical solutions to the LaneEmden equation. *Physic Letters A* 2008; **372**:6060–6065.
19. Sajid M, Hayat T. Comparison of HAM and HPM methods in nonlinear heat conduction and convection equations. *Nonlinear Analysis*: *Real World Applications* 2008; **9**:2296–2301.
20. Liang S, Jeffrey DJ. Comparison of homotopy analysis method and homotopy perturbation method through an evolution equation. *Communications in Nonlinear Science and Numerical Simulation*, DOI: 10.1016/j.cnsns.2009.02.016.
21. Hayat T, Khan M. Homotopy solutions for a generalized second-grade fluid past a porous plate. *Nonlinear Dynamics* 2005; **42**:395–405.
22. Hayat T, Ellahi R, Asghar S. The influence of variable viscosity and viscous dissipation on the non-Newtonian flow: an analytical solution. *Communication in Nonlinear Science and Numerical Simulation* 2007; **12**:300–313.
23. Abbasbandy S, Yürüsoy M, Pakdemirli M. The analysis approach of boundary layer equations of power-law fluids of second grade. *Zeitschrift für Naturforschung A* 2008; **63a**:564–570.
24. Abdulaziz O, Hashim I. Fully developed free convection heat and mass transfer of a micropolar fluid between porous vertical plates. *Numerical Heat Transfer*, *Part A* 2009; **55**:270–288.

25. Abdulaziz O, Noor NFM, Hashim I. Homotopy analysis method for fully developed MHD micropolar fluid flow between vertical porous plates. *International Journal for Numerical Methods in Engineering* 2008; DOI: 10.1002/nme.2509.
26. Sami Bataineh A, Noorani MSM, Hashim I. Solution of fully developed free convection of a micropolar fluid in a vertical channel by homotopy analysis method. *International Journal for Numerical Methods in Fluids* 2008; DOI: 10.1002/fld.1918.